Supplementary Information for "Do Conformational Biases of Simple Helical Junctions Influence RNA Folding Stability and Specificity?"

Vincent B. Chu, Jan Lipfert, Yu Bai, Vijay S. Pande,
Sebastian Doniach, Daniel Herschlag

August 26, 2009

Stochastic Dynamics (SD) simulation of a multi-scale model of the tethered duplex using Gromacs

In the hierarchical model of RNA folding, the flexibility of the junction regions is the dominant influence on the conformational ensemble of the helices, which are treated as as collection of rigid bodies. To account for this in our modeling, we created multiscale representations of the dPEG and sPEG constructs by coarse-graining the helices while retaining atomistic detail in the junction regions (Fig. 1).

In our multiscale representations, each helix is replaced by a collection of "dummy" atoms and fiducial atoms that allow us to replace the coarse-grained helices with their atomistic representations. Each dummy atom (blue atoms aligned along the helical axis in Fig. 1) was assigned a Van der Waals radius of 4 Å. Parameters for the bond lengths, angles, and dihedrals for the PEG linker were obtained from experimental studies [1, 2].

We used the Gromacs software package to conduct long stochastic dynamics simulations of the sPEG and dPEG constructs [3]. The great reduction in the number of atoms in the simulated construct resulted in a substantial decrease in the computational cost of the simulation. For each simulation, the friction constant for the SD simulation was set at 0.01 ps. Bonds and angles where held constant using the SHAKE algorithm.

We first began by equilibrating both constructs at 300 K for 1.6 μs. After this initial step, another simulation of 1.6 μs was conducted and ten evenly-spaced snapshots from this simulation were used to seed ten other simulations. From these ten simulations, snapshots of the constructs were taken every 16 ps of simulation time. The total number of recorded frames represents $\sim$45 μs of simulation for each construct. Convergence of the simulation was checked using block averaging (data not shown).

After the simulations were completed, the fiducial atoms in each recorded frame were used to fit atomistic representations of the helices creating a large set of atomic models for the sPEG and dPEG constructs. Structures with sterically incompatible configurations were excluded yielding a set of 290,300 and 299,900 sPEG and dPEG structures, respectively.

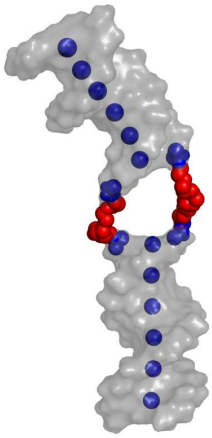

Supplementary Figure 1: Visualization of the multiscale model used to represent the dPEG construct (sPEG differs only by deletion of a single PEG tether). In the multiscale model, the helices (gray) are replaced by a set of dummy atoms aligned along the helices and fiducial atoms that uniquely specify the helical location and orientation (blue). The junction (red) is represented in all-atom detail.

Monitoring the Salt-Induced Structural Relaxation of the Tethered Duplex by SAXS

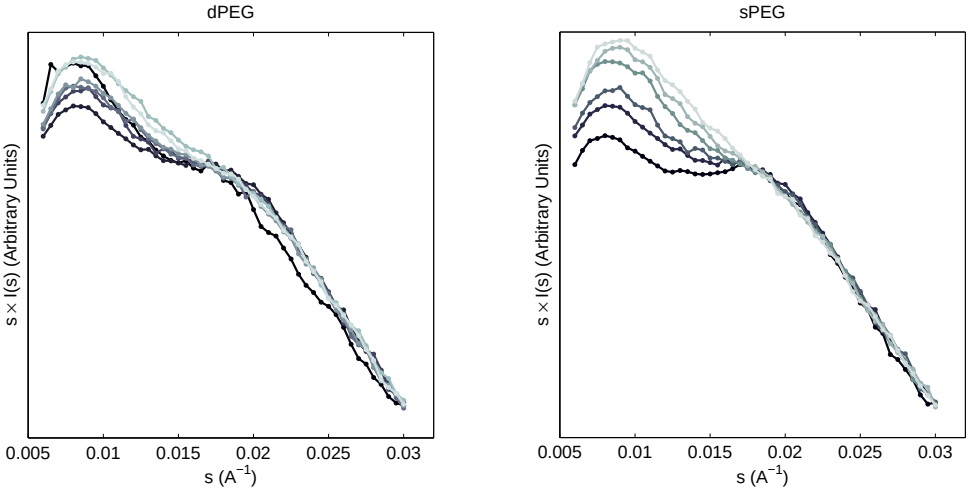

Supplementary Figure 2: Experimentally measured SAXS profiles for the dPEG (left) and sPEG (right) constructs plotted in the Holtzer representation over a range of salt concentrations. The superimposition of the profiles highlights the salt-induced transition from from an extended structure at 0.016 M (black) to a structurally relaxed structure at 1.016 M (light gray). The transition is less pronounced in the dPEG construct due to the addition of a second PEG tether and the smaller average helix-helix separation.

Electostatic Calculations using the Adaptive Poisson-Boltzmann Solver (APBS)

The electrostatic penalty for assembling the helices in a given configuration Ω was computed with the Adaptive Poisson-Boltzmann Solver (APBS v0.5.1) [4]. Charges and atomic radii were assigned for each of the atoms in each helix using PDB2PQR, a utility included in the standard APBS package [5].

Solutions to the nonlinear Poisson-Boltzmann (PB) equation were computed with boundary conditions set by the Debye-Hückel solution. The interior of the molecule was defined as the union of spheres centered on each atomic coordinate with radii equal to the sum of the van Der Waals radii and a solvent probe radius of 1.4 Å. The interior of the molecule was assigned a dielectric value of $\epsilon = 2.0$ while the exterior was assigned $\epsilon = 78.4$. Charges were assigned to grid points

using a cubic b-spline discretization. Grid resolution for all simulations was 0.5 Å.

Due to the high computational cost of repeated solutions of the PB equation, we did not compute an electrostatic energy for every helical configuration in the set $\{\Omega_j\}$. Instead, we assumed that the electrostatic energy for a given helical configuration was dependent only on the location and direction of the two helical axes (i.e., the electrostatic energy was insensitive to rotations of the helices about their respective axes). We then constructed a smaller set of helical configurations by first defining a set of 100 helical axes evenly distributed over the unit sphere; the mobile helix was then aligned to these axes and translated to 13,754 grid points spaced 2 Å apart in a box of size $52 \times 46 \times 46$ Å. The corner of the box was placed at $\mathbf{r} = (-14, -28, -28\,\text{Å})$. Configurations found to be sterically clashed were removed, yielding a set of 945,671 helical configurations. PB calculations were then computed on these configurations and interpolated to the full set of helical configurations found in $\{\Omega_j\}$.

References

[1] Bai, Y., V. Chu, J. Lipfert, V. Pande, D. Herschlag, and S. Doniach. 2008. Critical assessment of nucleic acid electrostatics via experimental and computational investigation of an unfolded state ensemble. *J. Am. Chem. Soc.* 130:12334–12341.

[2] Kienberger, F., V. Pastushenko, G. Kada, H. Gruber, C. Riener, H. Schindler, and P. Hinterdorfer. 2000. Static and Dynamical Properties of Single Poly(Ethylene Glycol) Molecules Investigated by Force Spectroscopy. *Single Molecules.* 1:123–128.

[3] Van Der Spoel, D., E. Lindahl, B. Hess, G. Groenhof, A. Mark, and H. Berendsen. 2005. GROMACS: fast, flexible, and free. *J Comput Chem.* 26:1701–1718.

[4] Baker, N., D. Sept, S. Joseph, M. J. Holst, and J. A. McCammon. 2001. Electrostatics of nanosystems: Applications to microtubules and the ribosome. *Proc. Natl. Acad. Sci. USA.* 98:10037–10041.

[5] Dolinsky, T. J., J. E. Nielsen, J. A. McCammon, and N. A. Baker. 2004. PDB2PQR: an automated pipeline for the setup of Poisson-Boltzmann electrostatics calculations. *Nucleic Acids Res.* 32:665–667.